Cerebral Cortex March 2015;25:667–679
doi:10.1093/cercor/bht258
Advance Access publication October 1, 2013

Functional Interactions Between Large-Scale Networks During Memory Search

James E. Kragel[1,2] and Sean M. Polyn[1]

[1]Department of Psychology and [2]Neuroscience Graduate Program, Vanderbilt University, Nashville, TN 37240, USA

Address correspondence to Sean M. Polyn, Vanderbilt University, Department of Psychology, PMB 407814, 2301 Vanderbilt Place, Nashville, TN 37240-7817, USA. Email: sean.polyn@vanderbilt.edu

Neuroimaging studies have identified two major large-scale brain networks, the default mode network (DMN) and the dorsal attention network (DAN), which are engaged for internally and externally directed cognitive tasks respectively, and which show anticorrelated activity during cognitively demanding tests and at rest. We identified these brain networks using independent component analysis (ICA) of functional magnetic resonance imaging data, and examined their interactions during the free-recall task, a self-initiated memory search task in which retrieval is performed in the absence of external cues. Despite the internally directed nature of the task, the DAN showed transient engagement in the seconds leading up to successful retrieval. ICA revealed a fractionation of the DMN into 3 components. A posteromedial network increased engagement during memory search, while the two others showed suppressed activity during memory search. Cooperative interactions between this posteromedial network, a right-lateralized frontoparietal control network, and a medial prefrontal network were maintained during memory search. The DAN demonstrated heterogeneous task-dependent shifts in functional coupling with various subnetworks within the DMN. This functional reorganization suggests a broader role of the DAN in the absence of externally directed cognition, and highlights the contribution of the posteromedial network to episodic retrieval.

Keywords: DMN, episodic memory, fMRI, free recall, functional connectivity

Introduction

In studies of the human memory system, when a specific external cue successfully prompts memory retrieval, functional magnetic resonance imaging (fMRI) techniques reliably identify a core network of brain regions spanning the hippocampal formation (HF), posterior cingulate (PC) cortex, posterior parietal cortex (PPC), and medial prefrontal cortex (mPFC; Shannon and Buckner 2004; Vincent et al. 2006; Spaniol et al. 2009). These regions belong to a brain network known as the "default mode network" (DMN). They show spontaneous correlation during resting states (Raichle et al. 2001), and exhibit increased activity during self-referential tasks (Buckner and Carroll 2007; Andrews-Hanna, Reidler, Sepulcre, et al. 2010; Qin and Northoff 2011), suggesting that these regions play a critical role in internally directed cognitive processes.

In contrast to the DMN, Corbetta and Shulman (2002) described the "dorsal attention network" (DAN), which is implicated in attentional orienting to external stimuli, and consists of dorsal parietal cortex including the intraparietal sulcus, and dorsal prefrontal cortex, including the putative frontal eye fields. These 2 networks are consistently anticorrelated during cognitive tasks requiring external attention (Fox et al. 2005). A study by Sestieri et al. (2011) illustrates this anticorrelation across tasks: While a perceptual search task engaged the DAN and suppressed the DMN, an episodic retrieval task engaged the DMN and suppressed the DAN. Guerin et al. (2012) explicitly varied the attentional and memorial difficulty of the test stimuli in a recognition paradigm, showing that even within-task, these networks exhibit competitive interactions, particularly within lateral parietal cortex. These findings support a bipartite view of cortical organization, in which distinct large-scale networks support internally and externally based cognitive processes (Binder et al. 1999; Greicius et al. 2003; Fox et al. 2005; Frank et al. 2005).

Recent human neuroimaging results challenge this bipartite organizational scheme, suggesting that the exclusively competitive nature of these networks is an artifact of the cognitive tasks used to examine their dynamics. For example, when an external cue is used to prompt recollection of source details of a particular experience, the DAN and DMN show cooperative interactions in the form of positive functional coupling (Simons et al. 2007; Fornito et al. 2012). Spreng et al. (2010) compared the dynamics of these networks during an autobiographical planning task and a visuospatial planning task, and found a functional reorganization between the two tasks. They identified a frontoparietal control (FPC) network that coupled with DMN when the task involved self-referential information, and coupled with DAN when the task involved visual information. While the autobiographical planning task of Spreng et al. (2010) is both goal-driven and internally directed, it yields subjective behavioral responses (regarding the fidelity and quality of the generated plans), limiting one's ability to link the neural dynamics of the DAN and DMN to the behavioral dynamics of memory retrieval.

Free recall is an excellent paradigm for examining the nature of DAN and DMN interactions during internally directed cognitive processes. This task is goal-driven, internally directed, and yields well-characterized behavioral responses regarding the particular contents of remembered experience. Participants study a series of items, and then are asked to vocally report those items in any order, without the aid of an external cue. A recent study by Shapira-Lichter et al. (2012) found a competitive interaction between DAN and DMN brain regions during free recall, supporting the bipartite view of cortical organization. While DAN regions showed strong activity early in the free-recall period which declined over the course of memory search, DMN regions were deactivated early in the period, showing a gradual recovery over the course of the search. Notably, Shapira-Lichter et al. (2012) did not observe recruitment of the same FPC network that coupled with the DMN in the autobiographical planning task reported by Spreng et al. (2010), suggesting that internally directed memory search may require a distinct network organization from internally directed planning.

We used a combination of network-based (using independent component analysis [ICA]) and region-based analysis to examine the dynamics of these large-scale functional networks as participants searched their memory during a free-recall

task. We observed a functional reorganization of the DMN during the recall period itself, with increased functional coupling between a posteromedial network, a right-lateralized FPC network, and a medial prefrontal network demonstrating spatial correspondence with the DMN. Our results suggest that memory retrieval in free recall involves increased coupling of attentional and memorial networks, reflecting reorganization of intrinsic connectivity.

Materials and Methods

Participants

We tested 20 (12 females) native English speakers between 18 and 35 years of age, after obtaining consent in accordance with procedures approved by the Vanderbilt University Institutional Review Board. Participants received payment of $20/h for their participation, with up to an additional $10 earned dependent upon performance in the task.

Experimental Procedure

Participants ran in a variant of the free-recall paradigm, in which they studied a sequence of 12 lists (spanning 2 separate sessions), each of which contained 24 study items. Stimuli were presented with a computer running *PyEPL* (Geller et al. 2007). After each study list, participants performed either a free-recall test or a source recognition test. Each session included 3 free-recall lists and 3 source recognition lists; the conditions were pseudorandomly ordered within each session. Here, we focus exclusively on the free-recall trials, depicted in a schematic representation in Figure 1*A*.

Each word was studied with a semantic orienting task (either a size judgment or an animacy judgment) requiring a keypress response from the participant. Prior to stimulus presentation, a cue appeared on the screen for 0.7 s in order to indicate which orienting task would apply to the upcoming stimulus. After presentation of the task cue, we displayed a fixation cross for an interval of 0.3 ± 0.1 s, followed by presentation of a study item for 2.5 s, during which the participant made their judgment. An interstimulus fixation interval between 0.5 and 5 s in duration followed each study item. We optimized the order of tasks and the duration of the interstimulus intervals to increase efficiency in estimation of the hemodynamic response to each task (Dale 1999), with the constraints that a task was not repeated more than 6 consecutive times, and that half of the items on a given list were studied in each of the 2 tasks.

After the final study item was presented on a given list, participants were given 75 s to freely recall as many items as they could remember from the most recent list, in any order. We recorded vocal responses using a scanner-safe voice recording system (Resonance Technologies, Inc.). Custom software (Cusack et al. 2005) and the "Noise Removal" tool in Audacity removed audio noise from the scanner from audio recordings. We scored vocalized responses offline using *PyParse* (Solway et al. 2010) and *Penn TotalRecall*.

Following the recall portion of the task, participants performed 1 of 3 control tasks: a speech control task, an eyes-open task, and an eyes-closed task. During the speech control task, words were presented in the same format as in the encoding period. Items presented during the speech task were presented for a duration of 2 s, with an interstimulus interval of 4 s. Participants were presented a total of 3 items per list, for a total of 18 speech trials. The eyes-open and eyes-closed tasks consisted of presentation of the auditory cues "open" and "close," which instructed the participant to either attend to the fixation cross, or close their eyes, respectively. Auditory cues were presented with an ISI of 10 s, with a total of 6 cues per functional run.

Each of the 20 participants performed 2 sessions of the free-recall paradigm in the 3 T Phillips MRI scanner at the Vanderbilt University Institute of Imaging Science. Prior to imaging sessions, participants performed 2 behavioral sessions for familiarization with the task, to ensure consistent behavioral performance during scanning.

Image Acquisition

Functional images were collected using an interleaved EPI pulse sequence (TR = 2000 ms, TE = 30 ms, voxel size = 3.0 × 3.0 × 3.6 mm, flip angle = 75°, FOV = 192 mm). During the functional EPI scans, 30 oblique slices were collected over the whole brain, oriented parallel to the AC-PC plane. Whole-brain MP-RAGE structural scans were collected (TR = 2500 ms, TE = 4.38 ms, voxel size = 1.0 × 1.0 × 1.0 mm, flip angle = 8°, FOV = 256 mm).

Image Processing

Preprocessing

The first 4 volumes of each functional run were removed to allow for equilibration of scanner signal. Preprocessing of fMRI data was

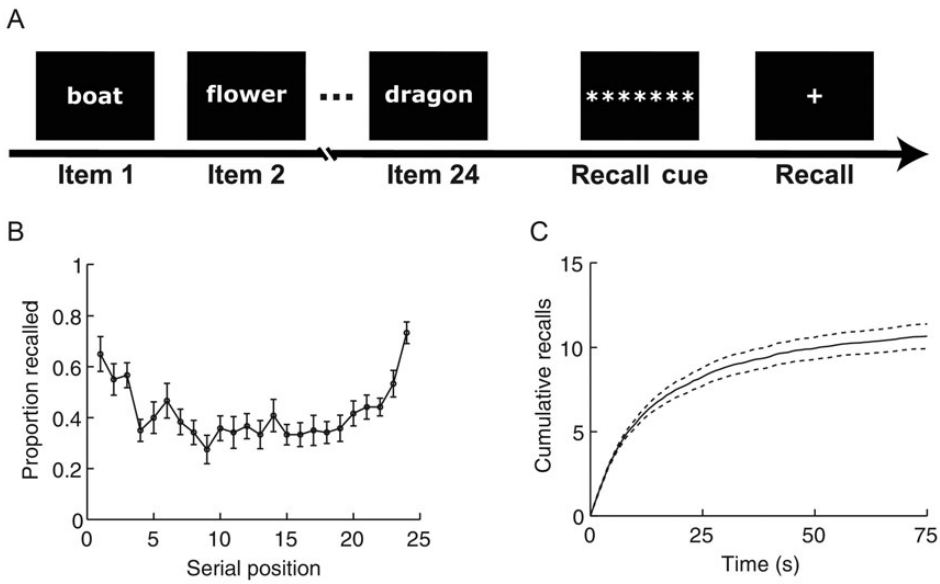

Figure 1. (*A*) Schematic representation of a free-recall trial used in the experiment. During the encoding period, participants were presented with a list of 24 items. Each encoding period was followed by a recall cue of 300 ms duration, followed by a 75-s recall period. (*B*) Mean recall (±1 SEM) performance as a function of serial position. (*C*) Cumulative distribution plot of recalls made across the recall period. Dotted lines represent SEM.

performed using routines as implemented by the SPM8 software package. All volumes from the 12 functional runs were realigned to the first functional volume of the first run, correcting for head motion. A mean functional image was generated from the realigned timeseries and co-registered to the T_1-weighted whole-brain anatomical scan. These T_1-weighted anatomical images were then segmented into gray matter, white matter, and cerebrospinal fluid, and normalized to a template in Montreal Neurological Institute (MNI) stereotactic space using the unified segmentation approach as implemented in the "New Segment" tool in SPM8 (Ashburner and Friston 2005). Images were resampled to 3-mm isotropic voxels and spatially smoothed with a 8-mm FWHM Gaussian kernel.

Independent Component Analysis

ICA was used to identify spatially distinct neural networks contributing to fMRI signal during the free-recall task, without assumption of a temporal model of hemodynamic activity. Independent networks were identified using the Group ICA of fMRI Toolbox (Calhoun et al. 2001). To reduce data complexity, principal component analysis was applied to each individual participants' data. The number of independent sources was estimated to be 28 using the minimum description length criterion (Li et al. 2007). Next, the resultant timeseries were concatenated across participants, and ICA was conducted using the Infomax algorithm. Time courses and spatial maps resulting from the ICA solution were back-projected for each individual participant. Timeseries amplitude was converted to percent signal for comparison across participants. Spatial loading of components was examined using a random-effects model, by performing 1-sample *t*-tests on the component maps, accounting for multiple comparisons (familywise error corrected, $P < 0.05$). Group component maps constructed in this manner were used in post hoc region-based analyses.

Rejection of Non-Neural Components

Use of ICA as an analytic tool has the benefit of identifying sources of noise in the BOLD timeseries. We employed an automated artifact removal method based on both anatomical and spatial constraints in the components (Sui et al. 2009). This method uses 2 criteria for component rejection based upon anatomical and geometric properties of the spatial maps. The gray matter and ventricular cerebrospinal fluid probabilistic atlases provided by SPM8 were correlated with the spatial map of each component, yielding 2 correlation values c_{GM} and c_{CSF}. Components of interest should be localized to gray matter, and as such, any components with $|c_{CSF}| > |c_{GM}|$ were rejected. The second criteria ensured the components were spatially clustered, as expected of physiological sources measured with fMRI. For each component map, we computed the focusing degree, defined as the ratio between the spatial entropy and the degree of clustering, the proportion of above threshold ($|t_{(19)}| > 6.51$) voxels within a 100-mm^3 cluster (for more details, see Formisano et al. 2002). The focusing degree was compared with a dynamically determined threshold, and components below the threshold were identified as artifacts.

Component Selection and General Linear Modeling

A general linear model (GLM) was constructed for the selection of ICs of interest, as well as subsequent post hoc analyses (e.g., psychophysiological interaction analysis). As described in Experimental Procedure, a single functional run can be decomposed into 3 periods: encoding, retrieval, and control tasks. As the present analyses focus on network dynamics during the free-recall task, any functional run in which a participant performed the source recognition task was omitted from further analysis. Three conditions of interest were incorporated into the model: transient recall events, a sustained event covering the duration of the entire recall period, and speech control events. Nine additional covariates were included within the model: encoding events, eyes-open events, eyes-closed events, and 6 motion parameters computed during image realignment. Regressors of interest were constructed by convolving a basis function at the time of an individual event onset, with the canonical hemodynamic response function and its temporal derivative as implemented in SPM8.

Transient recall events and speech events were modeled with Dirac delta functions, with a stimulus duration of 0 s, and onset at the initiation of the vocal response. The sustained recall condition was modeled with a duration of 75 s (the duration of the recall period) and onset coincident with presentation of the initiation cue. Encoding events were modeled with a duration of 3 s, with onsets placed coincident with presentation of the task cue. Eyes-open and eyes-closed events were modeled with a duration of 10 s, allowing for the construction of alternating block regressors.

The regression analysis produced estimated β-coefficients for transient recall (β_{Rt}), sustained recall (β_{Rs}), and speech (β_{Sp}) events for each participant. A linear contrast of transient and speech-related activity ($\beta_{Rt} - \beta_{Sp}$) was constructed to identify recall-related neural signals unrelated to speech production. A second-level "random-effects" analysis was performed using a 1-sample *t*-test to identify recall-related components across the group of participants, treating participant as a random factor.

Components (ICs) were considered task relevant if they exhibited either a significantly nonzero β_{Rt} or β_{Rs} at a threshold of $P < 0.05$ (Bonferroni corrected for the total number of non-noise components). It should be noted that this contrast identifies task-relevant activity versus the implicit baseline in the described GLM, which is comprised of passive fixation across the session, including intertrial intervals during encoding, as well as periods of rest between task periods (encoding, retrieval, and control tasks).

The study period included 2 distinct encoding tasks, which have previously been shown to influence neural activity both during the encoding and retrieval of items associated with each respective task (Polyn et al. 2012). We implemented an additional regression analysis, constructing separate transient recall regressors for the "size task" and "animacy task" separately. To ensure that the identified components reflected task-general activity, a conjunction analysis was implemented: any transient component must be significantly nonzero regardless of encoding task ($\beta_{Rt,size} > 0 \cap \beta_{Rt,animacy} > 0$).

To examine variability in the response of functional networks showing task-related profiles, we constructed a finite impulse response (FIR) model, using the same GLM as described above. The FIR basis set modeled activity ranging from 6 s prevocalization to 20 s postvocalization. The FIR window length was determined post hoc in order to maximize the efficiency in estimating the response at each timepoint, given the distribution of individual recall times (Öztekin et al. 2010). While the overlap in responses does introduce collinearity into the GLM and reduces overall power, it allows for the separation of neural activation that occurs leading up to, and concurrent with, individual retrieval events. Activity leading up to individual recall events is of interest, given prior studies demonstrating retrieval-related processing preceding individual recalls (Polyn et al. 2005; Gelbard-Sagiv et al. 2008).

Minimizing Motion-Related Signal

Overt speech production, as required by the free-recall and speech control tasks examined here, has been shown to increase head motion relative to covert speech (Barch et al. 1999). We implemented a number of measures in order to ensure the neural dynamics characterized in this study were not unduly influenced by motion-induced artifact. To minimize head motion in the scanner, padding was placed within the head coil around the participant's head, and the participant was given specific instructions to remain as still as possible while speaking.

Motion-related artifacts tend to have characteristic spatial profiles, with artifactual signal appearing near the edge of the skull, and at the boundaries of different tissue classes (Barch et al. 1999). Additionally, the inferior region of the brain is noticeably susceptible to magnetic field change caused by speaking, due to proximity to the mouth and throat (Birn et al. 1998). The ICA-based artifact rejection technique described above identifies ICs that were likely to have been artifactual in origin, and removes these components from the set of analyzed components (Beckmann et al. 2000; Sui et al. 2009).

In addition, we inspected incremental head motion during scanning, to ensure that no within-scan movement exceeded half the voxel size (>1.5 mm). Additionally, we ensured no within-scan rotation

exceeded 1.5°. Choice of these thresholds was determined based on visual inspection of the raw fMRI and participant motion timeseries. Even minimal head motion can produce a characteristic striped artifact when using interleaved slice acquisition. We visually inspected the global fMRI signal over the course of the experimental session to identify such artifacts. If a participant exhibited such an artifact during a given scan (regardless if it was coincident with subject motion), an additional binary regressor was added to that participant's GLM to remove the effects of artifactual variances on the regression analyses. A total of 3 participants exceeded this within-scan movement threshold. Within this subset of the data, the total number of TRs exhibiting large amounts of within-scan motion or motion-related artifact was minimal (range of 1–3 TRs per subject). Similar methods have been implemented in dealing with high-movement clinical populations (Mazaika et al. 2009).

To ensure that the identified components reflected cognitive rather than motion-related signal, we included estimated motion parameters as a covariate of interest in all GLM-based analyses. Finally, prior work has shown that certain motion-induced artifacts arising from overt speech production are variable in terms of their spatial location across participants (Barch et al. 1999). The group-based analyses employed here will tend to minimize the influence of these artifacts.

Network Correspondence Analysis

To identify the correspondence between the observed ICs and large-scale networks that have been observed in low-frequency spontaneous fluctuations in BOLD signal, we performed a correlation-based correspondence analysis. For each IC, we computed the Pearson product-moment correlation between the group-averaged spatial map (thresholded at $t > 3$) and masks corresponding to 7 (binary) cortical network maps constructed by Yeo et al. (2011). Voxels contained in the intersection of the 2 images were included in the computation. It should be noted that the resting state network templates are restricted to the cortical mantle, and deep brain structures such as the hippocampus and basal ganglia are excluded. Network templates used in this analysis include the dorsal attention, ventral attention, default mode, FPC, somatomotor, visual, and limbic networks (for details, see Yeo et al. 2011).

Network Interaction Analysis

Spontaneous (Task-Unrelated) Network Interactions

We implemented a partial correlation analysis, after accounting for variability in the BOLD response due to recall-related activity, to estimate spontaneous (i.e., task-unrelated) functional connectivity of pairs of regions. First, we applied a low-pass filter ($f < 0.08$ Hz) to each of the component timeseries engaged during the free-recall task. For each pairwise combination of the components of interest, functional coupling was estimated as the partial correlation of the noise-corrected component timeseries, while controlling for the effects of the remaining 3 component timeseries, as well as the task regressors constructed in the basic GLM. This procedure allowed for the isolation of interactions that were specific to each network pair, and could not be explained by a common response to the task.

Task-Related Network Interactions

To analyze changes in coupling between the functional networks identified using ICA, we implemented a correlational psychophysiological interaction analysis (Fornito et al. 2012). It should be emphasized that this analysis examines the effective connectivity between the identified ICs, and tests for changes in coupling resulting from specific events during the cognitive task. By focusing on the coupling of networks, rather than specific regions of interest (ROIs), analyses of this nature have provided insight into the organization and interactions of large-scale functional networks (Sridharan et al. 2008; St Jacques et al. 2011).

This analysis identifies components whose covariation changes as a function of task state, by modeling main effects of the psychological task, physiological signal, and their interaction. It controls for any correlations that may arise from either spontaneous or independent coactivation effects by including timeseries representing both the component of interest, as well as the predicted activity associated with the free-recall task. The remaining interaction term provides a measure of task-related changes in functional coupling between the timeseries of interest. For each of the component timeseries of interest, we computed the interaction effect using a deconvolution technique (Gitelman et al. 2003). For each pairwise combination of the networks of interest, we calculated the partial correlation between the interaction effects, while controlling for component timeseries and modeled task effects. Given violations of normality in observed measures of functional coupling, we implemented nonparametric tests in the form of Wilcoxon signed-rank and rank-sum tests to determine significant interactions across participants.

Regions of Interest Analysis

We constructed ROIs by identifying, within each component map, clusters composed of contiguous voxels within a priori anatomical ROIs using the Automated Anatomical Labeling toolbox (Tzourio-Mazoyer et al. 2002). Anatomical ROIs included association cortex within the prefrontal cortex (PFC), parietal cortex, and medial temporal lobe (i.e., we excluded the occipital lobe, lateral temporal cortex, pre- and postcentral gyri, and the cerebellum). Anatomical information concerning the constructed ROIs can be found in Supplementary Materials. We extracted the average signal within each cluster, and modeled the signal using linear regression as previously described (see component selection and GLM). This analysis yielded estimates for a sustained recall-related component (β_{Rs}), a transient recall-related component (β_{Rt}), and a speech-related (β_{Sp}) component, for each ROI. Statistical testing of ROI timeseries was implemented under the same framework as the component identification analysis, with Bonferroni correction calculated based on the total number of ROIs.

Results

Behavioral Results

Overall, the proportion of items recalled by participants was 0.42 (SEM 0.03). Figure 1*B* shows the serial position curve observed when probability of recall was calculated as a function of list position. We observed a primacy effect (increased recall for serial positions 1–3 relative to serial positions 4–21 [$t_{(19)} = 5.31$, $P < 0.0001$]), and a recency effect (increased recall for serial positions 22–24 relative to serial positions 4–21 [$t_{(19)} = 5.91$, $P < 0.0001$]). Figure 1*C* characterizes the timing of participants' recall responses; as the recall period progresses, the number of recalls made increased in a negatively accelerating manner, with a mean inter-response time (IRT) of 5.09 s (SEM 1.21 s). A more thorough description of the behavioral effects observed in this experiment can be found in a prior publication examining patterns of task-related activity in these data (Polyn et al. 2012).

Speech-Induced Head Motion

We characterized speech-induced head motion with 1-way repeated-measures ANOVAs, with the computed incremental motion parameters as the dependent variable, task (e.g., encoding, recall, and speech) as the independent variable, and subject as an additional factor. Despite subject motion increasing numerically during the speech and control tasks, as shown in Table 1, this increase was not statistically significant for any of the comparisons (all $P > 0.05$). Nevertheless, we include estimates of subject motion as covariates in the following regression-based analyses to ensure the observed patterns of activity are not unduly influenced by non-neural signal sources.

Table 1
Differences in head motion are compared across 3 separate task conditions

		Encoding	Recall	Speech
Translations (mm)	*X*	0.013 (0.11)	0.0089 (0.15)	0.006 (0.18)
	Y	0.033 (0.11)	0.045 (0.16)	0.069 (0.18)
	Z	0.019 (0.24)	−0.084 (0.38)	−0.024 (0.36)
Rotations (degrees)	Roll	0.059 (0.29)	0.17 (0.45)	0.039 (0.52)
	Pitch	0.012 (0.11)	−0.0057 (0.18)	−0.031 (0.19)
	Yaw	0.0099 (0.14)	−0.025 (0.19)	−0.023 (0.22)

Across-subject incremental averages are reported, with the standard deviation in parenthesis.

Imaging Results

Functional Networks Engaged During Recall

The free-recall paradigm presents a challenge to standard analysis techniques, in that the timing of the responses are determined by the behavior of the subject (Öztekin et al. 2010), and the timing of hemodynamic response relative to the behavioral response is unknown. Spatial ICA (Calhoun et al. 2001) provides a data-driven technique that characterizes the temporal dynamics and spatial distribution of functional networks, and has been shown to identify functional networks that are present during both task-related cognition and rest (Smith et al. 2009). We applied this technique to the neural signal recorded during free-recall periods, and identified a set of components related to memory search. To this end, we constructed 2 sets of regression coefficients, one designed to identify sustained component activity related to memory search (a block regressor rising for the entire free-recall period and flat otherwise), and one designed to identify transient component activity related to memory search (delta functions corresponding to the individual recall vocalizations). Both sets of coefficients were convolved with a standard hemodynamic response function. This analysis identified one independent component (IC) exhibiting a sustained positive response during memory search, 7 ICs showing a sustained negative response, 4 ICs exhibiting transient positive responses, and one IC showing a transient negative response, from among the full set of components. Here, we describe the 5 positive-going components (sustained and transient); in the next section, we describe the negative-going components.

We assign a descriptive name to each of these 5 networks, based on the most prominent brain regions identified within it. A full accounting of the regions associated with each network is provided in Supplementary Table 2. IC_6 (posteromedial, PM) included bilateral medial temporal lobe structures (including hippocampus), retrosplenial cortex (RSC), and ventromedial prefrontal cortex (vmPFC). This network was identified as having a sustained response during free recall, using the above-mentioned regression analysis (β_{Rs} significantly >0; $t_{(19)}=4.38$, $P<0.008$). Previous studies examined a network with similar structure that was shown to activate during declarative (Vincent et al. 2006) and autobiographical (St Jacques et al. 2011) memory tasks. A subset of these regions are part of the DMN, which shows increased activation when mental images are constructed from mnemonic representations (Hasselmo et al. 2007; Andrews-Hanna, Reidler, Sepulcre, et al. 2010).

The first transiently responding network (significantly nonzero β_{Rt} across subjects; $t_{(19)}=3.94$, $P<0.02$) was IC_7 (dorsal frontoparietal, DFP), which contained bilateral PFC (including bilateral dorsolateral PFC, and left lateralized rostrolateral PFC), bilateral supramarginal gyrus, and precuneus. Previous studies have implicated a similar network in top-down cognitive control processes (Badre and Wagner 2007; Vincent et al. 2008). The second transiently responding network (positive β_{Rt}; $t_{(19)}=11.88$, $P<0.0001$) was IC_{12} (temporoinsular, TI), which covered the superior temporal gyrus, Heschl's gyrus, middle temporal gyrus, insula, and anterior cingulate cortex. Previous studies have implicated similar regions in tasks involving speech execution, verbal feedback (Christoffels et al. 2007) and auditory perception, specifically speech processing (Binder et al. 2000). The third transient network (positive β_{Rt}; $t_{(19)}=4.39$, $P<0.008$) was IC_{13} (cerebellar, CER), which spans the cerebellum and portions of dorsolateral PFC. The final transient network (positive β_{Rt}; $t_{(19)}=13.17$, $P<0.0001$) was IC_{24} (somatomotor, SM), which included bilateral somatomotor cortex, striatum, and superior cerebellum. Previous studies have implicated a similar network during execution of overt speech (Huang et al. 2001; van de Ven et al. 2009).

For each of the transiently responding components, we contrasted activity during recall events to activity during a speech production task, to determine whether fluctuations in activity were better thought of as speech-related or recall-related. The DFP and CER networks showed a reliably smaller response during the speech control task as compared with recall events (DFP/IC_7: $t_{(19)}=6.24$, $P<0.0001$; CER/IC_{13}: $t_{(19)}=3.92$, $P<0.009$). In addition to being reliably activated during recall, the SM network was reliably activated during speech production ($t_{(19)}=7.45$, $P<0.0001$), and recall-related activity was not reliably stronger than speech ($t_{(19)}=-1.32$, $P>.99$).

Functional Networks Disengaged During Recall

A single component, IC_{20} (ventral prefrontal, VP), transiently decreased in activity during recall events relative to baseline (negative β_{Rt}; $t_{(19)}=-6.56$, $P<0.0001$). Six networks exhibited sustained deactivation across the recall period, including 2 of the 4 networks exhibiting transient positive responses relative to recall events: DFP/IC_7 (negative β_{Rs}; $t_{(19)}=-8.83$, $P<0.0001$), TI/IC_{12} (negative β_{Rs}; $t_{(19)}=-6.57$, $P<0.0001$).

This analysis identified 3 other components exhibiting sustained deactivation across the recall period. The first deactivated component (negative β_{Rs}; $t_{(19)}=-3.62$, $P<0.05$) was IC_{14} (right frontoparietal, RFP). Two additional networks exhibited deactivation: IC_{23} (PC) showed sustained decreases during memory search (negative β_{Rs}; $t_{(19)}=-7.01$, $P<0.0001$), as well as IC_{26} (medial prefrontal, MP: negative β_{Rs}; $t_{(19)}=-5.83$, $P<0.0001$). Figure 2 depicts the spatial distribution (top row) and temporal dynamics (bottom row) of the ICs exhibiting sustained differences in activity during memory search. These temporal profiles are averaged across all recall periods for all subjects, and provide a coarse view of when during the recall period the corresponding network shows maximal activity.

Network Correspondence Analysis

Given the known correspondence between large-scale functional networks identified using intrinsic measures of functional coupling during rest and task-based activation patterns (Smith et al. 2009), we next sought to identify the degree to which the identified ICs correspond to resting-state networks. Yeo et al. (2011) published spatial templates of 7 large-scale functional networks identified during resting periods with

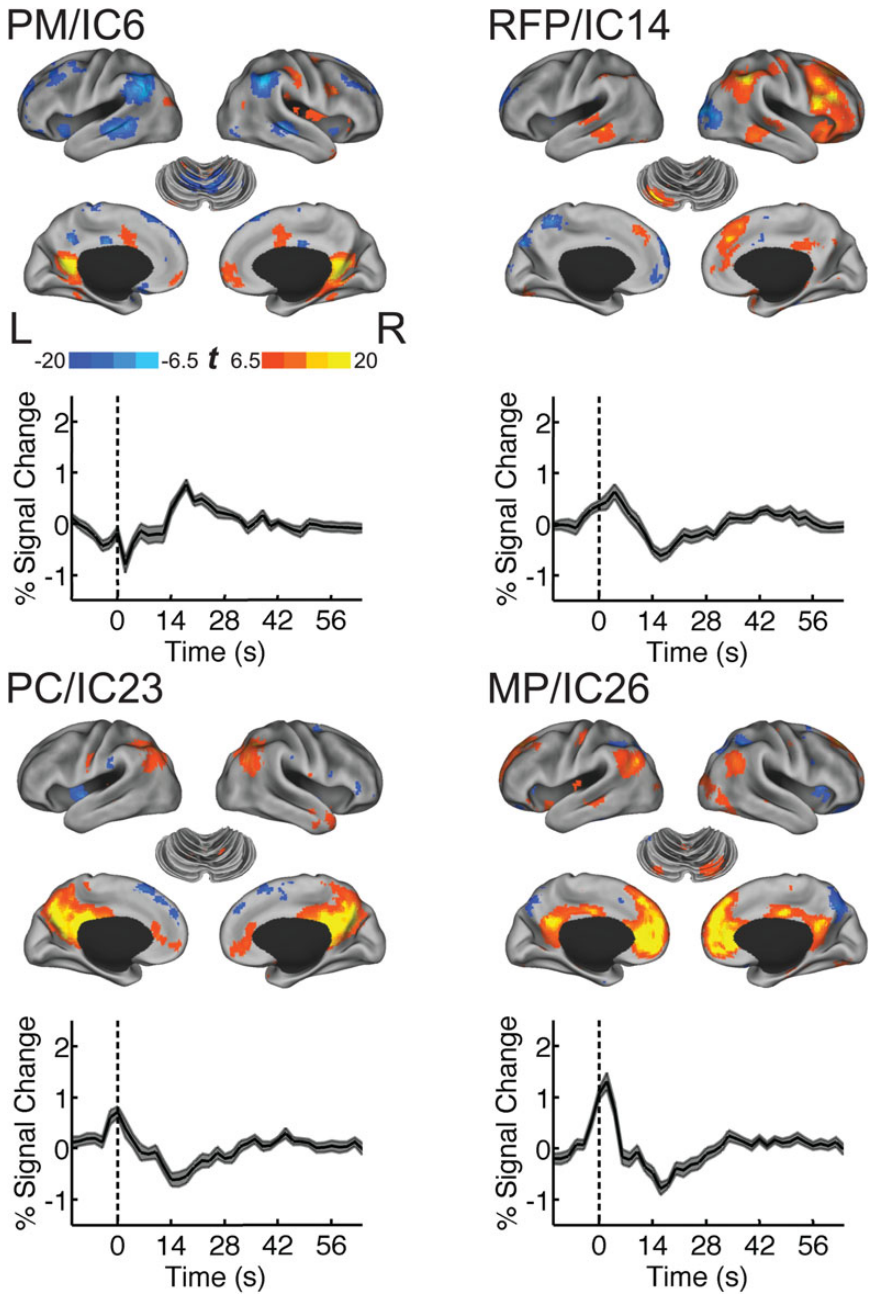

Figure 2. Large-scale functional networks exhibiting sustained changes in activity during self-initiated memory search. Component *t* maps are projected onto the inflation population average landmark surface (PALS) using CARET software (Van Essen et al. 2001). The mean component timeseries across the recall period, averaged across subjects, is depicted below each component map. The beginning of the recall period is marked at time point 0, indicated with the dashed vertical line. Shaded regions represent ±1 SEM.

fMRI, allowing us to quantify the correspondence between these networks and our ICs, using a Pearson product-moment correlation statistic.

A number of ICs showed a one-to-one correspondence with resting state networks. Three components showed a strong correspondence with the DMN, including PM/IC_6 ($r = 0.20$, $P < 0.0001$), PC/IC_{23} ($r = 0.29$, $P < 0.0001$), and MP/IC_{26} ($r = 0.45$, $P < 0.0001$). We observed a high degree of spatial correspondence between SM/IC_{24} and the somatomotor network ($r = 0.48$, $P < 0.0001$). RFP/IC_{14} exhibited a high degree of spatial correspondence with the FPC network ($r = 0.28$, $P < 0.0001$). DFP/IC_7 was the sole component identified with spatial similarity to the DAN ($r = 0.28$, $P < 0.0001$).

Of the task-relevant ICs, three did not demonstrate a clear one-to-one mapping with the resting state networks. VP/IC_{20} demonstrated moderate correspondence between both the DMN ($r = 0.22$, $P < 0.0001$) and the limbic network ($r = 0.37$, $P < 0.0001$). Despite the lack of a one-to-one mapping, a Hotelling–Williams test revealed significantly greater correlation between VP/IC_{20} and the limbic network than the DMN ($t_{(12981)} = 8.21$, $P < 0.0001$). TI/IC_{12} showed functional correspondence to both the somatomotor network ($r = 0.30$,

$P < 0.0001$) as well as the ventral attention network ($r = 0.22$, $P < 0.0001$). The magnitude of the correlation between TI/IC_{12} and the somatomotor network was greater than its correlation with the ventral attention network ($t_{(12981)} = 5.51$, $P < 0.0001$). CER/IC_{13} showed functional correspondence to both the visual network ($r = 0.12$, $P < 0.0001$) as well as the ventral attention network ($r = 0.12$, $P < 0.0001$). These correlation values were not significantly different from one another ($t_{(12981)} = 0.06$, $P > 0.47$).

Recall-Locked Analysis Reveals a Cascade of Engagement

In order to examine the dynamics of these components in the time surrounding each recall event, we constructed a FIR model for each component exhibiting transient activation during memory search, relative to the onset of the vocal response for each recall event. Figure 3 depicts the average response within multiple large-scale networks, from 6 s before to 20 s after vocalization onset. These event-averaged responses confirm the transient nature of the DFP, TI, CER, SM, and VP networks.

Furthermore, the FIR analysis reveals that these networks are engaged in a cascade relative to the recall onset. The temporal ordering of engagement was not specified or predicted by the regression analysis used to identify the components. We characterized the temporal order of engagement statistically by comparing, for pairs of components, the latency of the peak response across participants. The earliest peak was in the DFP/IC_7 network, which led the SM/IC_{24} network ($t_{(19)} = 3.66$, $P < 0.002$). The peak response within the SM network reliably lagged the CER/IC_{13} network ($t_{(19)} = 3.27$, $P < 0.004$). A summary of the statistically reliable peak latency differences is provided in Table 2. While variability in the hemodynamic response limits one's ability to resolve the relative timing of neural activity using fMRI, this variability is greater across

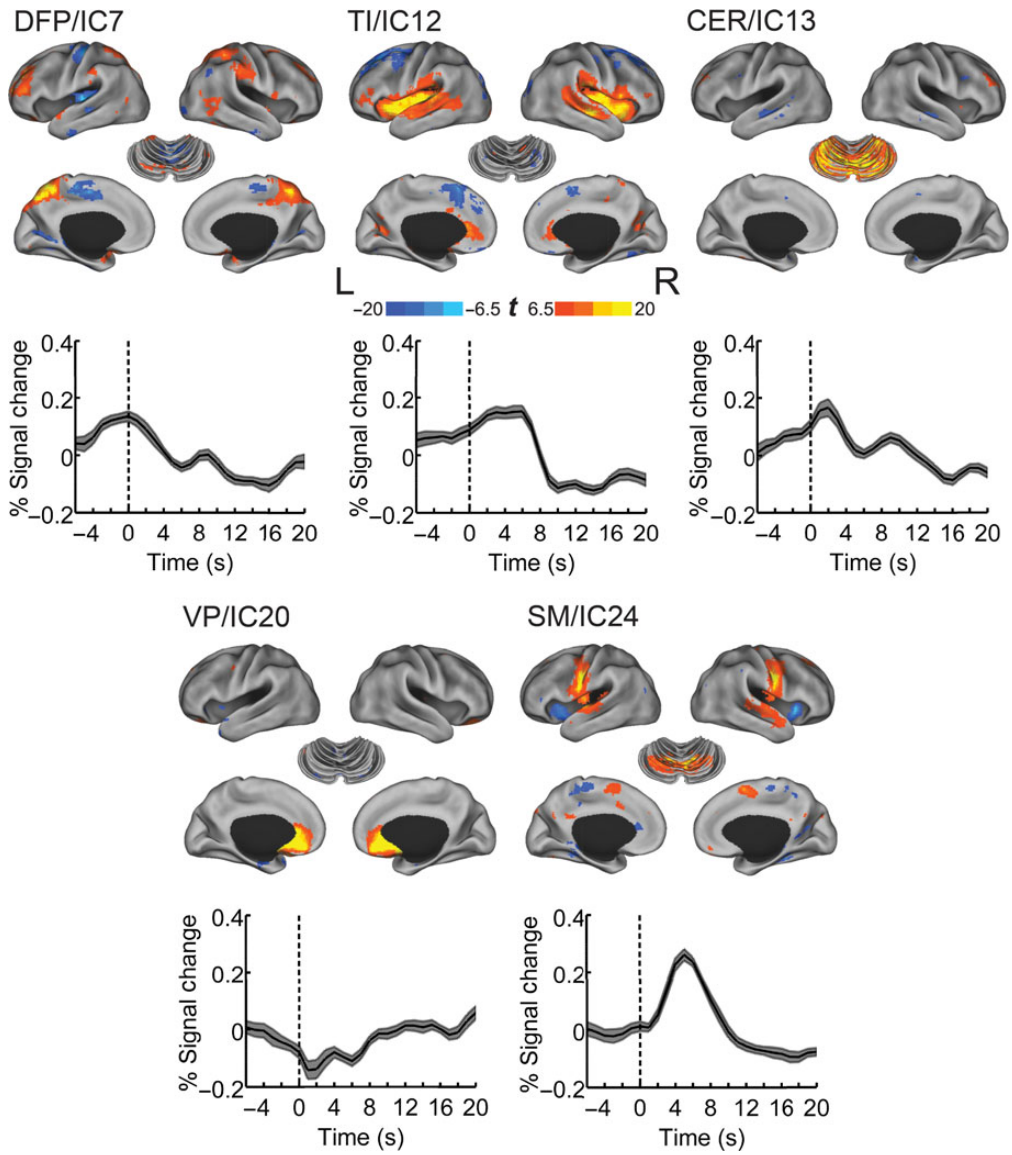

Figure 3. Large-scale functional networks exhibiting transient changes in activity locked to individual recall events. The top row depicts component *t* maps projected onto the inflation population average landmark surface (PALS) using CARET software (Van Essen et al. 2001). The time course of each component relative to the onset of recall vocalization (dashed vertical line), estimated using a finite impulse response model applied to the component time-series is depicted below each respective component map. Shaded regions represent ±1 SEM.

Table 2
Differences in peak latency of event-averaged signal across components (mean ± standard error) in seconds

	DFP/IC_7	TI/IC_{12}	CER/IC_{13}	SM/IC_{24}
DFP/IC_7		−3.1 ± 0.02	−1.65 ± 0.14	−4.8 ± 1.31*
TI/IC_{12}			1.45 ± 1.53	−1.7 ± 0.01
CER/IC_{13}				−3.15 ± 0.01*

*$P < 0.05$ Bonferroni corrected for multiple comparisons.

subjects than across cortical regions (Handwerker et al. 2004). Given the magnitude of the observed differences in peak latencies between components, these findings potentially reflect differences in the onset of neural activity. Regardless, confirmatory findings using modalities with superior temporal resolution (e.g., electrocorticography) are necessary to validate temporal or causal dependency between these networks.

Large-Scale Network Interactions During Memory Search

Network analysis of neural activity suggests that the brain is organized into competitive, large-scale functional brain networks (Fox et al. 2005). A classic example is the trade-off between the DMN, which engages during self-referential activity and disengages during attentional shifts to salient external stimuli (Andrews-Hanna, Reidler, Huang, et al. 2010), and attentional networks that show the converse pattern (Dosenbach et al. 2006; Fox et al. 2006). Computational models of human memory (Polyn and Kahana 2008) suggest that frontal and MTL regions should cooperate during self-initiated retrieval, but are presently too abstract to predict the nuanced temporal dynamics of this interaction.

In the present work, we implemented a partial correlation analysis to characterize the pairwise interactions of the 5 networks comprised of cortical regions commonly associated with either the DAN, DMN, or FPC networks (as identified in our network correspondence analysis). This analysis identifies correlations in spontaneous network activity, after accounting for variance correlated with the task structure (as modeled in the GLM). Spontaneous (i.e., not explicitly related to task regressors, which include regressors for recall events) interactions exhibited themselves both in terms of competition (a negative correlation in spontaneous activity) and cooperation (a positive correlation in spontaneous activity). All spontaneous network interactions are depicted in Figure 4*A*. The PM/IC_6 network exhibited a competitive interaction with the DFP/IC_7 network ($Z = -3.70$, $P < 0.002$), and a cooperative interaction with the MP/IC_{26} ($Z = 3.88$, $P < 0.02$) network. Additionally, low-frequency spontaneous fluctuations in the DFP/IC_7 network negatively coupled with those in the RFP/IC_{14} network ($Z = -3.73$, $P < 0.002$).

To test the degree to which memory search influences the functional coupling between the identified large-scale networks, we implemented a PPI analysis examining differences in functional coupling sustained throughout the recall period. As depicted in Figure 4*B*, the PM/IC_6 network exhibited sustained increases in functional coupling across the recall period with both the RFP/IC_{14} ($Z = 3.35$, $P < 0.004$) and the MP/IC_{26} ($Z = 3.81$, $P < 0.001$) networks. The DFP/IC_7 network exhibited sustained decreases in functional coupling with PC/IC_{23} ($Z = -3.40$, $P < 0.007$). We observed significant coupling between MP/IC_{26} (which demonstrates spatial correspondence with the DMN),

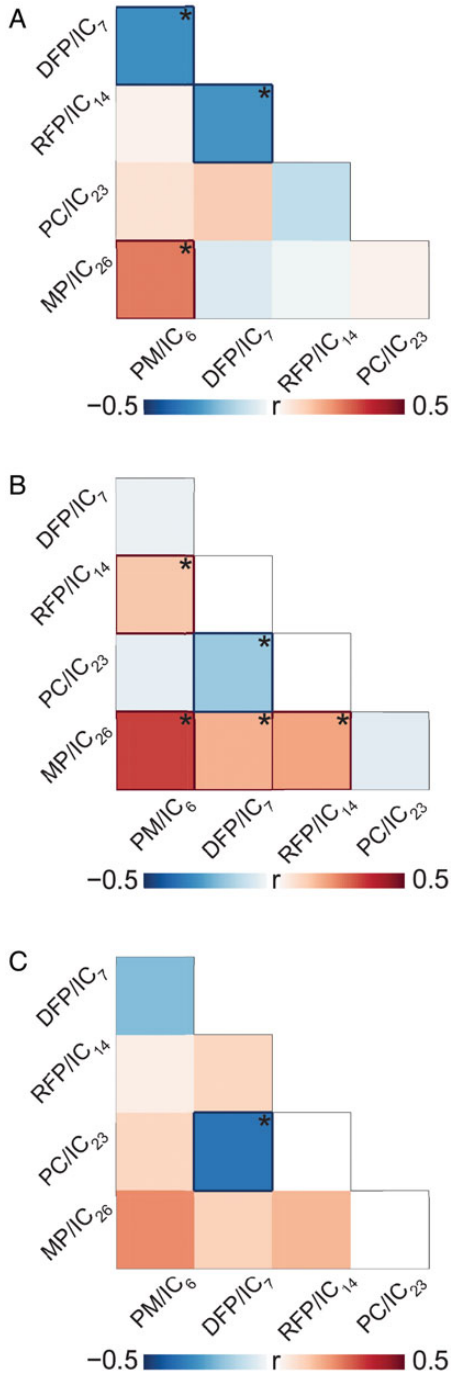

Figure 4. Interactions between functional networks. Distributions of (*A*) spontaneous, (*B*) sustained recall-related, and (*C*) transient recall-related connectivity. Cooperative and competitive network interactions are depicted in red and blue, respectively, with significance indicated with an asterisk ($P < 0.05$, Bonferroni-corrected).

and both DFP/IC_7 ($Z = 3.40$, $P < 0.007$) and RFP/IC_{14} ($Z = 3.02$, $P < 0.03$).

In addition to differences in functional coupling sustained throughout the recall period, we examined the degree to which functional connectivity between large-scale networks shifted during successful recall events by implementing an additional PPI analysis, constructing the interaction term based on the transient recall regressor. As shown in Figure 4*C*,

of all network interactions, only DFP/IC_7 and PC/IC_{23} demonstrated significant coupling ($Z = -3.14$, $P < 0.017$). To ensure that observed differences in network interactions are not attributable to response production alone, an additional PPI analysis was implemented by examining the interaction between large-scale network activity during the speech production task. Anticorrelation between DFP/IC_7 and PC/IC_{23} was stronger during recall than the speech control task ($Z = -3.15$, $P < 0.016$).

A number of network pairs demonstrated an increase in functional coupling during the recall period, when compared with spontaneous coupling: PM/IC_6 and DFP/IC_7 ($Z = 3.72$, $P < 0.002$), DFP/IC_7 and RFP/IC_{14} ($Z = 4.26$, $P < 0.0002$), DFP/IC_7 and MP/IC_{26} ($Z = 4.04$, $P < 0.0005$), and RFP/IC_{14} and MP/IC_{26} ($Z = 3.45$, $P < 0.006$). Only the DFP/IC_7 and PC/IC_{23} networks demonstrated stronger anticorrelation during the recall period ($Z = -4.36$, $P < 0.0001$).

Regional Analysis of the DMN, DAN, and FPC Networks

The neural theory surrounding the existence of large-scale brain networks supposes that that hemodynamic activity in a particular neuroanatomical region can be simultaneously influenced by multiple networks. If these networks exert opposing effects on the region, one will observe a difference between the dynamics observed in the raw BOLD response in that region, and the dynamics suggested by the network components. We performed an anatomically restricted ROI analysis in order to characterize potential discrepancies between BOLD response and component timeseries for particular neuroanatomical regions. From each group component map, we constructed ROIs using the Automated Anatomical Labeling toolbox (Tzourio-Mazoyer et al. 2002). Within each ROI, we constructed a mean hemodynamic response across voxels, and examined the neural response of the region using the same linear regression framework described above to identify task-related components.

We first examined ROIs whose BOLD activity was influenced by multiple task-sensitive ICs, including regions within PC cortex, PPC, and vmPFC. Spatial overlap of ICs was observed bilaterally within the lateral parietal cortex, in a cluster centered within angular gyrus (see: Supplementary Fig. 1). The task-sensitive components PC/IC_{23} and MP/IC_{26} contributed substantially to signal in these ROIs. These components showed sustained reductions during memory search, which were reflected in sustained deactivations within the superior parietal lobule ($t_{(19)} = -5.92$, $P < 0.0005$), and left angular gyrus ($t_{(19)} = -4.10$, $P < 0.03$). In contrast to inferior PPC ROIs, the ROI within the superior parietal lobule demonstrated increased activity during transient recall events, when compared with the speech control task ($t_{(19)} = 5.72$, $P < 0.0009$).

Spatial overlap of components was also observed within the vmPFC, mPFC, and RSC, with PM/IC_6, PC/IC_{23}, and MP/IC_{26} explaining variability within these regions. Transient increases during recall events relative to the speech control task were observed within mPFC ($t_{(19)} = 4.15$, $P < 0.03$), vmPFC ($t_{(19)} = 4.36$, $P < 0.018$), and RSC ($t_{(19)} = 4.74$, $P < 0.008$). Of these regions, the vmPFC exhibited sustained differences in activity during the recall period, showing decreased activity relative to the implicit baseline ($t_{(19)} = -4.48$, $P < 0.01$).

Certain regions identified within these 3 functional networks (PM/IC_6, PC/IC_{23}, and MP/IC_{26}) consistently exhibited sustained BOLD deactivation during memory search, even in ROIs constructed from PM/IC_6, which itself exhibited sustained increases in activity during search. While these components share a common midline core network within mPFC and PC cortex, they varied spatially as well. Three ROIs unique to PM/IC_6 were identified within the inferior frontal gyrus (IFG), superior frontal gyrus (SFG), and HF. We observed sustained decreases in BOLD activity in the IFG ($t_{(19)} = -5.07$, $P < 0.004$), and SFG ($t_{(19)} = -5.41$, $P < 0.001$) during memory search. Both the IFG ($t_{(19)} = 4.25$, $P < 0.02$) and SFG ($t_{(19)} = 4.08$, $P < 0.04$) exhibited transient increases in activity during recall events, when compared with speech production. Activity within the HF demonstrated transient increases during recall events when compared with both the implicit baseline ($t_{(19)} = 4.25$, $P < 0.02$) and the speech control task ($t_{(19)} = 4.22$, $P < 0.03$).

ROIs constructed from DFP/IC_7 exhibited recall-related modulation of the BOLD response (shown in Supplementary Fig. 2). Within DFP/IC_7, ROIs within the SFG ($t_{(19)} = -5.52$, $P < 0.001$), rostral PFC (rPFC) ($t_{(19)} = -3.99$, $P < 0.04$), left PFC ($t_{(19)} = -6.44$, $P < 0.0002$), and SMG ($t_{(19)} = -4.15$, $P < 0.03$) exhibited sustained decreases in activity during memory search. Of these ROIs, the rPFC ($t_{(19)} = 4.22$, $P < 0.03$) and SFG ($t_{(19)} = 4.81$, $P < 0.007$) exhibited decreased activity during speech production relative to episodic recall.

Of the ROIs constructed within RFP/IC_{14}, clusters within the left intraparietal sulcus ($t_{(19)} = -6.53$, $P < 0.0002$), right PPC ($t_{(19)} = -4.87$, $P < 0.005$), and right PFC (PFC_R; $t_{(19)} = -4.50$, $P < 0.01$) exhibited sustained deactivation during the free-recall task. Of these ROIs, transient recall-related effects (compared with the speech control task) were observed in both PFC_R ($t_{(19)} = 4.09$, $P < 0.03$) and PPC ($t_{(19)} = 4.11$, $P < 0.03$). One additional ROI within the HF exhibited transient effects comparing recall-related activity to baseline ($t_{(19)} = 5.08$, $P < 0.004$) and the speech control task ($t_{(19)} = 6.01$, $P < 0.0004$). A complete listing of all 53 ROIs, including anatomical coordinates and retrieval-related effects can be found in the Supplementary Material.

Discussion

We identified the contributions of multiple large-scale functional networks during self-initiated memory search, by applying ICA to fMRI while subjects performed a free-recall task. Multiple regression techniques were used to characterize how fluctuations in each component related to recall performance, and we observed unique recall-related signatures in several ICs consistent with the DMN, DAN, and FPC network. These findings provide insight into the role of these networks during an internally directed memory search task, and provide novel constraints for their proposed roles in cognition.

Fractionation of the DMN During Memory Search

We identified 3 networks that demonstrated spatial correspondence with the DMN; however, only the PM/IC_6 network increased in engagement during memory search. In contrast, PC/IC_{23} and MP/IC_{26} demonstrated decreased activity sustained throughout the recall period. Both PM/IC_6 and MP/IC_{26} exhibited cooperative interactions with RFP/IC_{14} during memory search, replicating prior work showing enhanced coupling between FPC networks and the DMN during internally directed cognitive tasks (Spreng et al. 2010; Fornito et al.

2012). This functional organization during memory search highlights the flexibility of large-scale networks (Fornito et al. 2012). Additionally, networks that are commonly observed to be anticorrelated using measures of intrinsic functional coupling may demonstrate cooperative interactions during specific tasks, such as memory retrieval.

Recent studies examining the functional organization of the DMN have identified fractionation of this large-scale network during both memory search (Sestieri et al. 2011) and internally directed paradigms (Andrews-Hanna, Reidler, Huang, et al. 2010). In an attempt to dissociate regions of the DMN that provide a specifically mnemonic function, Shapira-Lichter et al. (2013) compared decreases in activity during internally directed search, in which subjects performed either semantic, episodic, or phonemic fluency tasks. Consistent with findings from the present data, regions within the DMN demonstrated selectivity for both of the episodic and semantic tasks. Findings of heterogeneous contributions of the DMN suggest that a bipartite (e.g., Fox et al. 2005; Golland et al. 2007) view of cortical organization is an oversimplification. The posteromedial network, while commonly coactivated with the DMN, is functionally distinct from this larger network during the free-recall task.

Retrosplenial and parahippocampal cortices have been proposed by Ranganath and Ritchey (2012) to form the core of a posteromedial system that is recruited during episodic simulation (Hasselmo et al. 2007) and spatial navigation (Burgess et al. 2007), and which represents information pertinent to temporal and other causal relationships within a certain context. While the current study cannot speak to the specific function of the observed PM network outside of engagement during the free-recall task, activity within this network may reflect the integration of retrieved contextual information, which can be used to guide memory search (Howard and Kahana 2002; Polyn et al. 2009). Intracranial recordings within the temporal lobes have identified the reactivation of patterns of activity that may represent contextual information (Manning et al. 2011). Future work will determine whether the topographic patterns of neural activity in the functional networks investigated here show dynamics characteristic of modern computational models of memory (Polyn and Kahana 2008; Polyn and Sederberg 2013).

DAN Engagement During Internally-Directed Memory Search

A single functional network demonstrated a significant degree of spatial correspondence with the DAN, DFP/IC_7. Consistent with theories of competitive interactions between the DAN and DMN (Fox et al. 2005), the anticorrelation between this network and PC/IC_{23} became more pronounced during successful retrieval. Despite anticorrelation between these 2 networks that have been proposed to mediate internally and externally directed information (Corbetta et al. 2008; Vincent et al. 2008; Spreng et al. 2010), this transient engagement of DFP/IC_7 may suggest a more general cognitive mechanism supported by this network.

While the network correspondence analysis revealed similarity between the DFP/IC_7 network and the DAN, differences exist between the cortical regions comprising these networks. First, the medial bank of the intraparietal sulcus is absent within DFP/IC_7, with PPC activity occurring near the midline. Additionally, while DFP/IC_7 contains spatial overlap with the DAN in the putative frontal eye fields, prefrontal activation within DFP/IC_7 extends well into anterior PFC, in cortical regions commonly implicated in FPC networks. We speculate that differences in the observed network activity reflect task demands. Given the internal, rather than external, demands of the free-recall task, the observed absence of activity within visual cortex is consistent with these theories. The shift toward more pervasive prefrontal activity within this network may reflect additional executive control processes required to maintain internal representations during retrieval. Recruitment of this network may reflect top-down modulation of internal representations, concurrently supported through activity within anterior PFC.

It has been hypothesized that the DMN and DAN represent two major divisions of functional processing in cortex, with both networks supporting endogenous and exogenous specific processing, respectively. We observed competitive interactions between the DFP/IC_7 and PC/IC_{23}, sustained throughout the recall period. The strength of this anticorrelation increased during the successful retrieval of individual items, when there were increased demands for action-based processing involved in the planning and execution of speech production. It should be noted that these interactions are likely to result from mnemonic or internally directed focus of the retrieval task, given the lack of a similar effect during the speech control task. These findings are consistent with increased functional connectivity between the dorsal PC cortex (a central hub in the DMN) and frontoparietal networks in the absence of a focused task (Leech et al. 2012). Despite these findings, the present data suggest that different subnetworks within the DMN are flexibly engaged according to task demands. In addition, positive coupling between the DFP/IC_7 and MP/IC_{26} is indicative that anticorrelation between the DMN and DAN is reflective of specific cognitive demands, rather than an intrinsic property of functional organization.

FPC Coupling with the DMN During Retrieval

Recent studies have identified cooperative functional interactions between FPC networks and the DMN during internally directed tasks (Fornito et al. 2012), and the DAN during externally directed tasks (Spreng et al. 2010). These findings suggest a role for these networks in regulating the amount of internally and externally directed information used to guide behavior. Given the goal-directed nature of free recall, the failure to observe increased activity within FPC networks is surprising. However, external stimuli often play an important role in the internally directed tasks used in prior studies, either indicating when subjects are required to make a response, or providing a cue stimulus to guide memory search. It is possible that FPC recruitment reflects cognitive control mechanisms required to mediate between external cue stimuli processed by the DAN, and internal/memorial representations of the DMN. Under such a framework, there would be no need for the FPC network to mediate DAN/DMN interactions in free recall, given the absence of task-relevant perceptual information during the recall period.

While we did not observe engagement of FPC networks during free-recall, the RPF/IC_{14} network functionally coupled with both the PM/IC_6 and MP/IC_{23} networks during memory search. These findings support theories of functional

organization that propose goal-directed internally mediated cognition is supported through the integration of information between the DMN and FPC networks. We demonstrate a novel contribution of the PM/IC_6 network during the free-recall task, which functionally couples with DMN and FPC networks. Future studies can be used to infer the role of this network during memory search, possibly arbitrating between the retrieval of contextual information (Burgess et al. 2001), and the reconstruction of the encoding context under which the items were studied (Schacter et al. 2007). It will be critical to determine whether recruitment of this network mediates retrieval during the FR task, or if it is epiphenomenal in nature.

Large-Scale Networks Influence Posterior Parietal Cortex Activity During Retrieval

The organization of resting-state networks within PPC has influenced theories of PPC function (Vincent et al. 2006, 2008). Specifically, functional coupling between inferior PPC and the medial temporal lobe has led to the development of theories purporting a variety of mnemonic roles for the angular gyrus. In the present data, the overall BOLD response in this region is dominated by two networks within the DMN, PC/IC_{23} and MP/IC_{26}, resulting in sustained decreases in activity during memory search. Furthermore, both IC and ROI based analyses failed to demonstrate transient increases in activity within the angular gyrus. These findings provide constraints for theories of the role of parietal cortex in memory retrieval.

Among theories of PPC function, the "attention to memory" (AtoM) account (Cabeza et al. 2008, 2011; Ciaramelli et al. 2008) explains retrieval-related activation within parietal cortex as a result of dissociable attention-based functions within dorsal and ventral parietal cortex. Activity within dorsal parietal cortex (ranging from the lateral bank of the intraparietal sulcus to superior parietal cortex) is proposed to support top-down attention engaged during memory search. By this framework, inferior parietal activity is thought to reflect bottom-up capture of attention by the recovery of mnemonically salient information. Under the assumptions of the AtoM model, the free-recall task should recruit dorsal parietal cortex during memory search (e.g., sustained during IRTs within the recall period), and ventral parietal cortex during the detection of retrieved content. Consistent with the AtoM model and recent meta analysis of parietal retrieval effects (Hutchinson et al. 2009), regions within anterior inferior parietal cortex, within the supramarginal gyrus, exhibited transient increases in activity during successful recall, when compared with a speech control task. We observed a different pattern of activity within PPC near the angular gyrus, which exhibited sustained deactivation during search. Such a dissociation across the rostrocaudal aspect of ventral parietal cortex poses a challenge to the AtoM model and similar frameworks (Cabeza et al. 2012). To account for this pattern of activity, we turn to alternative models of parietal lobe function during episodic retrieval.

The output buffer hypothesis (Wagner et al. 2005) describes the role of the inferior parietal cortex (i.e., the angular gyrus) as supporting the online maintenance of recollected information. Expanding upon this theory, Vilberg and Rugg (2008) propose that the angular gyrus serves as the neural locus for the episodic buffer, supporting the online maintenance of multimodal representation of retrieved episodic information. This theory is supported by sustained activation in angular gyrus when retrieved content must be maintained over a delay (Vilberg and Rugg 2012). The role of the angular gyrus may be akin to dorsal frontoparietal networks that support the maintenance of online information in working memory (Curtis and D'Esposito 2003). Recent multivariate neuroimaging studies provide evidence suggesting that these networks play a role in the support of, but not the representation of, information within working memory (Riggall and Postle 2012). The observed functional networks containing the angular gyrus demonstrated sustained deactivation during memory search; however, networks spatially consistent with the DMN (but not the PM network) exhibited a marked increase in activity leading up to the recall period, consistent with the role of this network in maintenance of episodic content. While this interpretation is based upon reverse inference (under the assumption that increased angular gyrus activation reflects the maintenance of retrieved episodic information), this finding could be used to theoretically constrain mechanistic models of memory search.

Conclusions

In summary, we identified multiple large-scale functional networks that show modulation in activity during self-initiated memory search. We build upon recent neuroimaging findings implicating the DMN and DAN in free recall (Shapira-Lichter et al. 2012, 2013). We extend these findings through the application of ICA, which fractionated the DMN into three components. While two of these components exhibited sustained decreases in activity during memory search, a network centered in posteromedial cortex exhibited sustained increases in activity. These findings highlight the heterogeneity of large-scale functional networks, which are flexibly recruited to accomplish task-specific goals. Despite their intrinsically competitive nature, the PM network and the DFP network exhibited task-dependent functional coupling to mediate retrieval during self-initiated memory search. Our findings propose a challenge to models suggesting an exclusively competitive nature between neural systems supporting episodic retrieval and external attention, and demonstrate the nuanced contributions of multiple large-scale networks modulated by the free-recall task.

Supplementary Material

Supplementary material can be found at: http://www.cercor.oxfordjournals.org/.

Funding

This work was supported by the National Science Foundation (grant number 1157432) and a Vanderbilt University Discovery grant.

Notes

The authors thank Michael Rugg and Andrea Greve for helpful discussions and feedback. They also thank the members of the Vanderbilt Computational Memory Lab, especially Neal Morton and Joshua McCluey, who were involved with the collection of these data. *Conflict of Interest*: None declared.

References

Andrews-Hanna JR, Reidler JS, Huang C, Buckner RL. 2010. Evidence for the default network's role in spontaneous cognition. J Neurophysiol. 104:322–335.

Andrews-Hanna JR, Reidler JS, Sepulcre J, Poulin R, Buckner RL. 2010. Functional-anatomic fractionation of the brain's default network. Neuron. 65:550–562.

Ashburner J, Friston KJ. 2005. Unified segmentation. NeuroImage. 26:839–851.

Badre D, Wagner AD. 2007. Left ventrolateral prefrontal cortex and the cognitive control of memory. Neuropsychologia. 45:2883–2901.

Barch DM, Sabb FW, Carter CS, Braver TS, Noll DC, Cohen JD. 1999. Overt verbal responding during fMRI scanning: empirical investigations of problems and potential solutions. NeuroImage. 10:642–657.

Beckmann C, Noble J, Smith S. 2000. Artefact detection in FMRI data using independent component analysis. NeuroImage. 11:S614.

Binder J, Frost J, Hammeke T, Bellgowan P, Springer J, Kaufman J, Possing E. 2000. Human temporal lobe activation by speech and nonspeech sounds. Cereb Cortex. 10:512.

Binder JR, Frost JA, Hammeke TA, Bellgowan PSF, Rao SM, Cox RW. 1999. Conceptual processing during the conscious resting state: a functional MRI study. J Cogn Neurosci. 11:80–93.

Birn RM, Bandettini PA, Cox RW, Jesmanowicz A, Shaker R. 1998. Magnetic field changes in the human brain due to swallowing or speaking. Magn Reson Med. 40:55–60.

Buckner RL, Carroll DC. 2007. Self-projection and the brain. Trends Cogn Sci. 11:49–57.

Burgess N, Barry C, O'Keefe J. 2007. An oscillatory interference model of grid cell firing. Hippocampus. 17:801–812.

Burgess N, Becker S, King J, O'Keefe. 2001. Memory for events and their spatial context: models and experiments. Philos Trans R Soc Lond B Biol Sci. 356:1493–1503.

Cabeza R, Ciaramelli E, Moscovitch M. 2012. Cognitive contributions of the ventral parietal cortex: an integrative theoretical account. Trends Cogn Sci. 16:338–352.

Cabeza R, Ciaramelli E, Olson I, Moscovitch M. 2008. The parietal cortex and episodic memory: an attentional account. Nat Rev Neurosci. 9:613–625.

Cabeza R, Mazuz YS, Stokes J, Kragel JE, Woldorff MG, Ciaramelli E, Olson IR, Moscovitch M. 2011. Overlapping parietal activity in memory and perception: evidence for the attention to memory model. J Cogn Neurosci. 23:3209–3217.

Calhoun V, Adali T, Pearlson G, Pekar J. 2001. A method for making group inferences from functional MRI data using independent component analysis. Hum Brain Mapp. 14:140–151.

Christoffels IK, Formisano E, Schiller NO. 2007. Neural correlates of verbal feedback processing: an fMRI study employing overt speech. Hum Brain Mapp. 28:868–879.

Ciaramelli E, Grady CL, Moscovitch M. 2008. Top-down and bottom-up attention to memory: a hypothesis (AtoM) on the role of the posterior parietal cortex in memory retrieval. Neuropsychologia. 46:1828–1851.

Corbetta M, Patel G, Shulman GL. 2008. The reorienting system of the human brain: from environment to theory of mind. Neuron. 58:306–324.

Corbetta M, Shulman G. 2002. Control of goal-directed and stimulus-driven attention in the brain. Nat Rev Neurosci. 3:201–215.

Curtis CE, D'Esposito M. 2003. Persistent activity in the prefrontal cortex during working memory. Trends Cogn Sci. 7:415–423.

Cusack R, Cumming N, Bor D, Norris D, Lyzenga J. 2005. Automated post-hoc noise cancellation tool for audio recordings acquired in an MRI scanner. Hum Brain Mapp. 24:299–304.

Dale AM. 1999. Optimal experimental design for event-related fMRI. Hum Brain Mapp. 8:109–114.

Dosenbach NU, Visscher KM, Palmer ED, Miezin FM, Wenger KK, Kang HC, Burgund ED, Grimes AL, Schlaggar BL, Petersen SE. 2006. A core system for the implementation of task sets. Neuron. 50:799–812.

Formisano E, Esposito F, Kriegeskorte N, Tedeschi G, Di Salle F, Goebel R. 2002. Spatial independent component analysis of functional magnetic resonance imaging time-series: characterization of the cortical components. Neurocomputing. 49:241–254.

Fornito A, Harrison BJ, Zalesky A, Simons JS. 2012. Competitive and cooperative dynamics of large-scale brain functional networks supporting recollection. Proc Natl Acad Sci. 109:12788–12793.

Fox MD, Corbetta M, Snyder AZ, Vincent JL, Raichle ME. 2006. Spontaneous neuronal activity distinguishes human dorsal and ventral attention systems. Proc Natl Acad Sci USA. 103: 10046–10051.

Fox MD, Snyder AZ, Vincent JL, Corbetta M, Essen DCV, Raichle ME. 2005. The human brain is intrinsically organized into dynamic, anticorrelated functional networks. Proc Natl Acad Sci USA. 102:9673–9678.

Frank MJ, Woroch B, Curran T. 2005. Error-related negativity predicts reinforcement learning and conflict biases. Neuron. 47:495–501.

Gelbard-Sagiv H, Mukamel R, Harel M, Malach R, Fried I. 2008. Internally generated reactivation of single neurons in human hippocampus during free recall. Science. 3:96–101.

Geller AS, Schleifer IK, Sederberg PB, Jacobs J, Kahana MJ. 2007. PyEPL: a cross-platform experiment-programming library. Behav Res Methods. 39:950–958.

Gitelman DR, Penny WD, Ashburner J, Friston KJ. 2003. Modeling regional and psychophysiologic interactions in fMRI: the importance of hemodynamic deconvolution. NeuroImage. 19: 200–207.

Golland Y, Bentin S, Gelbard H, Benjamini Y, Heller R, Nir Y, Hasson U, Malach R. 2007. Extrinsic and intrinsic systems in the posterior cortex of the human brain revealed during natural sensory stimulation. Cereb Cortex. 17:766–777.

Greicius MD, Krasnow B, Reiss AL, Menon V. 2003. Functional connectivity in the resting brain: a network analysis of the default mode hypothesis. Proc Natl Acad Sci USA. 100:253–258.

Guerin SA, Robbins CA, Gilmore AW, Schacter DL. 2012. Interactions between visual attention and episodic retrieval: dissociable contributions of parietal regions during gist-based false recognition. Neuron. 75:1122–1134.

Handwerker DA, Ollinger JM, D'Esposito M. 2004. Variation of BOLD hemodynamic responses across subjects and brain regions and their effects on statistical analyses. NeuroImage. 21:1639–1651.

Hasselmo ME, Giocomo LM, Zilli EA. 2007. Grid cell firing may arise from interference of theta frequency membrane potential oscillations in single neurons. Hippocampus. 17:1252–1271.

Howard MW, Kahana MJ. 2002. A distributed representation of temporal context. J Math Psychol. 46:269–299.

Huang J, Carr TH, Cao Y. 2001. Comparing cortical activations for silent and overt speech using event-related fMRI. Hum Brain Mapp. 15:39–53.

Hutchinson JB, Uncapher MR, Wagner AD. 2009. Posterior parietal cortex and episodic retrieval: convergent and divergent effects of attention and memory. Learn Mem. 16:343–356.

Leech R, Braga R, Sharp DJ. 2012. Echoes of the brain within the posterior cingulate cortex. J Neurosci. 32:215–222.

Li YO, Adali T, Calhoun VD. 2007. Estimating the number of independent components for functional magnetic resonance imaging data. Hum Brain Mapp. 28:1251–1266.

Manning JR, Polyn SM, Baltuch G, Litt B, Kahana MJ. 2011. Oscillatory patterns in temporal lobe reveal context reinstatement during memory search. Proc Natl Acad Sci USA. 108:12893–12897.

Mazaika P, Hoeft F, Glover GH, Reiss AL. 2009. Methods and software for fmri analysis for clinical subjects. In: 15th Annual Meeting of the Organization for Human Brain Mapping; 2009, June 3; San Francisco, CA.

Öztekin I, Long NM, Badre D. 2010. Optimizing design efficiency of free recall events for fMRI. J Cogn Neurosci. 22:2238–2250.

Polyn SM, Kahana MJ. 2008. Memory search and the neural representation of context. Trends Cogn Sci. 12:24–30.

Polyn SM, Kragel JE, Morton NW, McCluey JD, Cohen ZD. 2012. The neural dynamics of task context in free recall. Neuropsychologia. 50:447–457.

Polyn SM, Natu VS, Cohen JD, Norman KA. 2005. Category-specific cortical activity precedes retrieval during memory search. Science. 310:1963–1966.

Polyn SM, Norman KA, Kahana MJ. 2009. A context maintenance and retrieval model of organizational processes in free recall. Psychol Rev. 116:129–156.
Polyn SM, Sederberg PB. Forthcoming 2013. Brain rhythms in mental time travel. NeuroImage. http://dx.doi.org/10.1016/j.neuroimage.2013.06.084.
Qin P, Northoff G. 2011. How is our self related to midline regions and the default-mode network? NeuroImage. 57:1221–1233.
Raichle ME, MacLeod AM, Snyder AZ, Powers WJ, Gusnard DA, Shulman GL. 2001. A default mode of brain function. Proc Natl Acad Sci. 98:676–682.
Ranganath C, Ritchey M. 2012. Two cortical systems for memory-guided behaviour. Nat Rev Neurosci. 13:713–726.
Riggall AC, Postle BR. 2012. The relationship between working memory storage and elevated activity as measured with functional magnetic resonance imaging. J Neurosci. 32:12990–12998.
Schacter DL, Addis DR, Buckner RL. 2007. Remembering the past to imagine the future: the prospective brain. Nat Rev Neurosci. 8:657–661.
Sestieri C, Corbetta M, Romani GL, Shulman GL. 2011. Episodic memory retrieval, parietal cortex, and the default mode network: functional and topographic analyses. J Neurosci. 31:4407–4420.
Shannon BJ, Buckner RL. 2004. Functional-anatomic correlates of memory retrieval that suggest nontraditional processing roles for multiple distinct regions within posterior parietal cortex. J Neurosci. 24:10084–10092.
Shapira-Lichter I, Oren N, Jacob Y, Gruberger M, Hendler T. 2013. Portraying the unique contribution of the default mode network to internally driven mnemonic processes. Proc Natl Acad Sci. 110:4950–4955.
Shapira-Lichter I, Vakil E, Glikmann-Johnston Y, Siman-Tov T, Caspi D, Paran D, Hendler T. 2012. Inside out: a neuro-behavioral signature of free recall dynamics. Neuropsychologia. 50:2245–2256.
Simons JS, Henson RNA, Gilbert SJ, Fletcher PC. 2007. Separable forms of reality monitoring supported by anterior prefrontal cortex. J Cogn Neurosci. 20:447–457.
Smith SM, Fox PT, Miller KL, Glahn DC, Fox PM, Mackay CE, Filippini N, Watkins KE, Toro R, Laird AR et al. 2009. Correspondence of the brain's functional architecture during activation and rest. Proc Natl Acad Sci. 106:13040–13045.
Solway A, Geller AS, Sederberg PB, Kahana MJ. 2010. Pyparse: a semi-automated system for scoring spoken recall data. Behav Res Methods. 42:141–147.
Spaniol J, Davidson PS, Kim AS, Han H, Moscovitch M, Grady CL. 2009. Event-related fMRI studies of episodic encoding and retrieval: meta-analyses using activation likelihood estimation. Neuropsychologia. 47:1765–1779.
Spreng RN, Stevens WD, Chamberlain JP, Gilmore AW, Schacter DL. 2010. Default network activity, coupled with the frontoparietal control network, supports goal-directed cognition. NeuroImage. 53:303–317.
Sridharan D, Levitin DJ, Menon V. 2008. A critical role for the right fronto-insular cortex in switching between central-executive and default-mode networks. Proc Natl Acad Sci. 105:12569–12574.
St Jacques PL, Kragel PA, Rubin DC. 2011. Dynamic neural networks supporting memory retrieval. NeuroImage. 57:608–616.
Sui J, Adali T, Pearlson GD, Calhoun VD. 2009. An ICA-based method for the identification of optimal FMRI features and components using combined group-discriminative techniques. NeuroImage. 46:73–86.
Tzourio-Mazoyer N, Landeau B, Papathanassiou D, Crivello F, Etard O, Delcroix N, Mazoyer B, Joliot M. 2002. Automated anatomical labeling of activations in SPM using a macroscopic anatomical parcellation of the MNI MRI single-subject brain. NeuroImage. 15:273–289.
van de Ven V, Esposito F, Christoffels IK. 2009. Neural network of speech monitoring overlaps with overt speech production and comprehension networks: a sequential spatial and temporal ICA study. NeuroImage. 47:1982–1991.
Van Essen DC, Drury HA, Dickson J, Harwell J, Hanlon D, Anderson CH. 2001. An integrated software suite for surface-based analyses of cerebral cortex. J Am Med Inform Assoc. 8:443–459.
Vilberg KL, Rugg MD. 2008. Memory retrieval and the parietal cortex: a review of evidence from a dual-process perspective. Neuropsychologia. 46:1787–1799.
Vilberg KL, Rugg MD. 2012. The neural correlates of recollection: transient versus sustained fMRI effects. J Neurosci. 32:15679–15687.
Vincent JL, Kahn I, Snyder AZ, Raichle ME, Buckner RL. 2008. Evidence for a frontoparietal control system revealed by intrinsic functional connectivity. J Neurophysiol. 100:3328–3342.
Vincent JL, Snyder AZ, Fox MD, Shannon BJ, Andrews JR, Raichle ME, Buckner RL. 2006. Coherent spontaneous activity identifies a hippocampal-parietal memory network. J Neurophysiol. 96:3517–3531.
Wagner A, Shannon B, Kahn I, Buckner R. 2005. Parietal lobe contributions to episodic memory retrieval. Trends Cogn Sci. 9:445–453.
Yeo BTT, Krienen FM, Sepulcre J, Sabuncu MR, Lashkari D, Hollinshead M, Roffman JL, Smoller JW, Zöllei L, Polimeni JR et al. 2011. The organization of the human cerebral cortex estimated by intrinsic functional connectivity. J Neurophysiol. 106:1125–1165.